GMR
The Original

SUSTAINABLE GREEN FABRICATION OF MULTISCALE POLYMERIC NANOCOMPOSITE FROM *Padina tetrastromatica*: A STRUCTURAL INSIGHT INTO WOUND HEALING POTENTIAL ON HaCaT CELLS MODEL

Vishal Suraj Ravindran[1], Manodhar Naidu Vunnam[2], Ramganesh Selvarajan[3]*

[1]Saveetha Medical College & Hospital (SMCH), Saveetha Institute of Medical and Technical Sciences (SIMATS), Thandalam, Chennai, Tamil Nadu 602105, India. klssvishal@gmail.com
[2]Department of Nephrology, Saveetha Medical College and Hospital, Saveetha Institute of Medical And Technical Sciences (SIMATS), Thandalam, Chennai-602105, Tamil Nadu, India. Email: manodharnaidu9@gmail.com
[3]Centre for Microbial Ecology and Translational Research, Department of Microbiology, Saveetha Medical College and Hospital, Saveetha Institute of Medical And Technical Sciences (SIMATS), Thandalam, Chennai-602105, Tamil Nadu, India.
Email: ramganesh.presidency@gmail.com
*Corresponding Author: ramganesh.presidency@gmail.com (R.S.)

ABSTRACT
This study reports the green synthesis of copper oxide nanoparticles (CuO NPs) using *Padina tetrastromatica* algal extract and their incorporation into starch/polyvinyl alcohol (PVA) electrospun nanocomposite for enhanced wound healing applications. UV-Vis spectroscopy confirmed CuO NP formation via a distinct surface plasmon resonance (SPR) peak at 273 nm, while Fourier-transform infrared spectroscopy (FTIR) analysis revealed characteristic Cu–O bonds (602.84 cm^{-1}) and residual bioactive compounds from the extract. X-ray diffraction (XRD) confirmed the monoclinic tenorite phase of CuO NPs, whereas Scanning electron microscopy (SEM) imaging demonstrated uniform nanoparticle dispersion within a porous, fibrous scaffold matrix. Thermogravimetric analysis (TGA) indicated thermal stability up to 300°C, and Dynamic light scattering (DLS) analysis revealed a hydrodynamic diameter of ~108 nm with a zeta potential of −22.13 mV, suggesting colloidal stability. The wound healing scratch assay on HaCaT keratinocytes demonstrated that starch/PVA/CuO-NP nanocomposite significantly accelerated wound closure (95.65% at 100 µg/mL) compared to CuO NPs (83.65%) and algal extract (69.65%) alone. Enhanced cell migration was attributed to the synergistic effects of the nanocomposite bioactive composition and structural properties. These findings highlight the potential of starch/PVA/CuO-NP nanocomposite as an advanced multifunctional wound dressing material, combining biocompatibility, structural integrity, and therapeutic efficacy.

KEYWORDS: *Padina tetrastromatica*, Green synthesis, CuO NPs, Starch/PVA/CuO-NPs nanocomposite, Wound-healing activity.

1. INTRODUCTION
Wound healing is a complex physiological process that involves a well-orchestrated sequence of events, including hemostasis, inflammation, proliferation, and tissue remodeling [1]. Disruptions in these stages, particularly in patients with chronic diseases such as diabetes or vascular disorders, can result in delayed healing and increased risk of infection [2]. To address these challenges, researchers have turned to advanced biomaterials that can not only support tissue regeneration but also provide antimicrobial and anti-inflammatory benefits [3]. Among these, nanotechnology has gained significant attention, particularly in the fabrication of nanostructured scaffolds that mimic the natural extracellular matrix (ECM) and facilitate cell adhesion, migration, and proliferation [4]. Electrospun nanofibrous scaffolds have emerged as promising platforms for wound dressing applications due to their high surface area-to-volume ratio, porosity, and mechanical properties conducive to tissue regeneration [5]. Biopolymer-based nanocomposite are at the forefront of wound healing innovations, particularly those incorporating biodegradable and biocompatible materials such as starch and polyvinyl alcohol (PVA) [6]. Starch, a naturally occurring polysaccharide, offers inherent biocompatibility, biodegradability, and moisture retention properties [7]. However, its mechanical limitations necessitate blending with other polymers, such as PVA, which imparts structural integrity and flexibility [8]. The synergistic combination of starch and PVA in electrospun nanofibers yields a biocompatible matrix with favorable physicochemical properties for biomedical applications [9]. Moreover, integrating therapeutic agents such as metal oxide nanoparticles into these nanofibers can further enhance their functionality, especially in combating microbial infections and accelerating wound repair [10].
Copper oxide nanoparticles (CuO NPs) have garnered attention due to their excellent antimicrobial, antioxidant, and pro-angiogenic properties, which are vital for effective wound healing [11]. Traditional chemical and physical synthesis methods for CuO NPs, however, often involve toxic solvents and hazardous reducing agents, raising concerns about their environmental and biological safety [12]. To overcome these limitations, green synthesis has emerged as a sustainable and eco-friendly alternative [13]. This approach utilizes biological entities such as plant

or algal extracts, which are rich in reducing and stabilizing agents like phenolics, flavonoids, terpenoids, and polysaccharides [14]. These biomolecules not only facilitate the reduction of metal ions but also cap the nanoparticles, enhancing their stability and biological activity [15].

Marine macroalgae, particularly brown seaweeds, are known to be rich sources of bioactive compounds with diverse therapeutic properties [16]. *Padina tetrastromatica*, a brown macroalga commonly found along the Indian coastline, has been reported to contain a wide array of bioactive constituents including fucoidans, laminarins, phlorotannins, and polyphenols [17]. These compounds possess potent antioxidant, antimicrobial, and anti-inflammatory properties, making *P. tetrastromatica* an ideal candidate for the green synthesis of nanoparticles [18]. Moreover, the use of ultrasound-assisted extraction (UAE) enhances the yield and efficiency of bioactive compound recovery from marine algae by disrupting cell walls and promoting solvent penetration through acoustic cavitation [19].

In this context, the present study was undertaken to develop and evaluate a novel, multifunctional electrospun nanofibrous scaffold composed of starch and PVA, embedded with CuO NPs synthesized via an ultrasonic-assisted green approach using *P. tetrastromatica* extract [20]. The primary objectives of this research were to harness the therapeutic potential of *P. tetrastromatica*-mediated CuO NPs and integrate them into biopolymer-based nanofibers to create a scaffold with enhanced physicochemical properties and biological efficacy [6]. The use of electrospinning as a fabrication technique allows for the production of nanofibers that closely mimic native ECM architecture, thereby offering an ideal microenvironment for cellular activities involved in wound healing [21].

The biosynthesis of CuO NPs using *P. tetrastromatica* extract offers multiple advantages [22]. It not only eliminates the need for hazardous reagents but also imparts intrinsic bioactivity to the nanoparticles, derived from the phytoconstituents in the algal extract [14]. The ultrasonic-assisted extraction process was carefully optimized to preserve the functional integrity of these bioactives, ensuring maximum therapeutic potential [23]. Following biosynthesis, the CuO NPs were incorporated into a starch/PVA matrix to fabricate nanofibrous scaffolds via electrospinning [24]. The selection of PVA as a synthetic polymer partner to starch was guided by its film-forming ability, biodegradability, and compatibility with electrospinning processes [25].

Comprehensive physicochemical characterization was performed to evaluate the structural, morphological, and thermal properties of both the synthesized CuO NPs and the final electrospun scaffolds [26]. Techniques such as UV-Vis spectroscopy, Fourier-transform infrared spectroscopy (FTIR), X-ray diffraction (XRD), Scanning electron microscopy (SEM), Thermogravimetric analysis (TGA), and dynamic light scattering (DLS) were employed to confirm nanoparticle formation, ascertain functional group interactions, analyze crystallinity, and assess the thermal stability and size distribution of the formulations [27]. These analyses confirmed the successful synthesis and integration of CuO NPs within the nanofiber matrix and provided insights into the scaffolds' suitability for biomedical applications [28].

In addition to physicochemical characterization, biological evaluation was conducted through *in vitro* wound healing assays using HaCaT keratinocyte cell lines [29]. The scratch assay method was employed to assess the migratory behavior of cells treated with varying concentrations of the algal extract, biosynthesized CuO NPs, and composite starch/PVA/CuO nanocomposite [30]. The results demonstrated enhanced wound closure rates and cell migration in samples treated with the composite scaffolds, indicating their potential to accelerate wound healing through synergistic antimicrobial and bioactive effects [31].

This research introduces a sustainable and biologically potent wound healing platform by integrating green-synthesized CuO NPs into starch/PVA-based electrospun nanocomposite. The study underscores the potential of marine macroalgae such as *P. tetrastromatica* as valuable bioresources for nanoparticle synthesis, and highlights the promise of nanotechnology-driven approaches in the development of next-generation wound dressings. The fabricated nanocomposite, characterized by their multifunctionality, biocompatibility, and enhanced therapeutic performance, present a significant advancement in the field of regenerative medicine and wound care.

2. MATERIALS AND METHODS

2.1. Materials

The brown macroalga *P. tetrastromatica* was sourced from the coastal waters of Rameswaram, Tamil Nadu, India, for the eco-friendly synthesis of CuO NPs. Copper(II) sulfate pentahydrate ($CuSO_4 \cdot 5H_2O$; Sigma-Aldrich) served as the precursor salt for nanoparticle formation. PVA, with an approximate molecular weight of 115,000, was used as the base polymer for nanofiber fabrication. Locally available native starch was included to improve the structural resilience of the scaffolds. All other reagents, such as ethanol and Milli-Q water (Merck, Sigma-Aldrich), were analytical grade. Nanofibers were fabricated using a HOLMARC HO-NFES-040 electrospinning apparatus with an integrated syringe pump. The samples were characterized through UV-Vis spectroscopy (VIS SPEC V-730), FTIR (PerkinElmer Spectrum Two), XRD (Bruker D8 Advance), SEM (JEOL JSM-IT800 NANO), DLS and zeta potential analysis (Malvern Zetasizer Ultra), and TGA (PerkinElmer TGA 8000). HaCaT keratinocytes cells were obtained from the National Centre for Cell Science (NCCS), Pune, India, which provided authenticated and contamination-free cell stocks for biological investigations focused on wound healing activity.

2.2. Marine macroalgae collection

Hand-harvested *P. tetrastromatica* specimens were collected from intertidal areas along the Rameswaram coast. The collected *Padina tetrastromatica* was taxonomically identified and authenticated by Dr V. Veeragurunathan, CSIR-CSMCRI-Marine Algal Research Station, Mandapam Camp 623519, Tamil Nadu, India. A voucher specimen was prepared and deposited at the Herbarium of the CSIR-CSMCRI-Marine Algal Research Station, under the accession number: SI–2025–RMM–015. This authentication ensures botanical accuracy and standardization of the study material. After collection, the biomass was initially rinsed with tap water to eliminate sediment, epiphytes, and debris, and then repeatedly washed with distilled water to remove salt and surface contaminants. Roughly 100 grams of cleaned seaweed were chopped into small pieces to support uniform drying. The samples were air-dried for two weeks in a shaded and well-aerated environment to preserve their bioactive components. Once fully desiccated, the algae were ground using a mechanical grinder into a fine, uniform powder to standardize particle size for downstream applications.

2.3. UAE

To extract bioactives, 2 g of powdered *P. tetrastromatica* were mixed in 50 mL of Milli-Q water. This solution was subjected to sonication in a LABQUEST ultrasonic water bath (Borosil; Serial No. 941032329018) at 60°C for 45 minutes. The ultrasound-assisted cavitation broke cell walls, promoting efficient release of intracellular contents. Following treatment, the solution was brought to ambient temperature and filtered using sterile Whatman No. 1 filter paper. The clear filtrate was refrigerated at 10°C for immediate use, and a portion was freeze-dried and sealed for long-term preservation and nanoparticle synthesis [32, 33].

2.4. Biosynthesis of CuO NPs

CuO NPs were produced via a green synthesis method, utilizing the algal extract as both reducing and stabilizing agents. A quantity of 10 mg freeze-dried extract was dissolved in 10 mL Milli-Q water, then added to 50 mL of 0.1 M $CuSO_4 \cdot 5H_2O$ in a 5:1 volume ratio. The solution was stirred continuously at 650 rpm and maintained at 60°C for 2 hours. A visible change from blue to bluish-green indicated Cu^{2+} ion reduction and nanoparticle formation. The precipitated CuO NPs were isolated via centrifugation, washed thoroughly with distilled water to eliminate residual impurities, and subsequently freeze-dried for 48 hours. The resulting powder was stored in a desiccator for further study [34].

2.5. Electrospinning of CuO-Starch/PVA nanofibers

To fabricate composite nanofibers, a 15% (w/w) aqueous PVA solution was prepared and stirred until completely dissolved. Then, 100 mg of native starch and 100 mg of CuO NPs were added into the polymer solution. The mixture was heated to 50°C and stirred continuously for 2.5 hours to ensure a homogeneous dispersion. The resulting uniform solution was transferred into a syringe fitted with a stainless steel needle (0.84 mm inner diameter) and mounted on a HOLMARC HO-NFES-040 electrospinning setup. Electrospinning parameters were optimized as follows: voltage of 11.5 kV, a tip-to-collector distance of 12.3 cm, and a flow rate of 0.4 mL/h. Electrospinning was performed at ambient conditions for 6–8 hours. The obtained fiber mats were peeled from the aluminum foil and stored in a desiccator until further use [35-37].

2.6. Characterization of nanoparticles and nanofiber scaffolds

2.6.1. UV-visible spectroscopy

The UV-Vis absorption spectrum of the biosynthesized CuO NPs was measured using a VIS SPEC V-730 spectrophotometer across the wavelength range of 200–800 nm. Deionized water was used as the reference. Peaks indicative of surface plasmon resonance confirmed successful nanoparticle synthesis [38].

2.6.2. FTIR analysis

FTIR spectra for the CuO NPs and composite fibers were collected using a PerkinElmer Spectrum Two FTIR with an ATR module. Spectra were recorded from 4000 to 400 cm^{-1} at a resolution of 4 cm^{-1}, averaging 64 scans per sample. Observed peaks corresponding to hydroxyl, phenolic, carboxylate, and Cu–O vibrations affirmed the incorporation of functional groups and nanoparticles into the polymer matrix [39].

2.6.3. XRD analysis

Crystalline properties and phase composition of CuO NPs and scaffolds were assessed using a Bruker D8 Advance X-ray diffractometer with CuKα radiation (λ = 1.5406 Å). Measurements ranged from 5° to 90° 2θ with a step size of 0.029649°, operating at 40 kV and 40 mA. Obtained patterns were compared with JCPDS standards to confirm CuO crystallinity and scaffold integration [40].

2.6.4. SEM analysis

The fiber morphology and nanoparticle integration were analyzed using a JEOL JSM-IT800 NANO SEM. Prior to imaging, the samples were gold-sputtered to improve conductivity. SEM images displayed a continuous fibrous structure with well-distributed nanoparticles and interconnected porosity, indicating proper scaffold formation [41].

2.6.5. TGA analysis

Thermal degradation behavior was examined via a PerkinElmer TGA 8000. Around 5 mg of each specimen was heated from room temperature to 550°C at a rate of 15°C/min under a nitrogen atmosphere. The weight loss profile

highlighted different degradation stages, such as moisture loss, polymer decomposition, and inorganic residue retention, revealing thermal stability [42].

2.6.6. Particle size and zeta potential

DLS and zeta potential measurements were carried out using a Malvern Zetasizer Ultra to assess the particle size distribution and surface charge. The high zeta potential values confirmed colloidal stability, suggesting minimal aggregation in aqueous suspension [27].

All experimental data, including raw and analyzed results, are available on the Mendeley Data repository (DOI:10.17632/ddbgcpm32x.2).

2.7. Wound healing (scratch) assay

The scratch assay was implemented to determine the cell migratory response of HaCaT keratinocytes following treatment with test agents: algal extract, CuO NPs, and starch/PVA/CuO nanofibers. Cells were plated into 12-well plates at a density of 2×10^5 cells/well in DMEM supplemented with 10% FBS and 1% penicillin-streptomycin, incubated at 37 °C in a humidified 5% CO_2 atmosphere until monolayers formed. A sterile 200 µL pipette tip created linear scratches simulating wounds. Wells were rinsed with PBS to remove cell debris. Treatments were applied in serum-free DMEM at concentrations of 6.25, 12.5, 25, 50, and 100 µg/mL. Untreated wells served as controls. Images were taken at 0, 24, and 48 hours using a phase-contrast microscope. ImageJ software quantified migration rates and calculated wound closure percentages to compare treatment effectiveness [43].

2.8. Statistical analysis

Statistical computations were carried out using SPSS version 25.0 and GraphPad Prism 9.0. Data from triplicate experiments were presented as mean ± standard deviation. Group comparisons were made using one-way ANOVA, followed by post-hoc tests such as Tukey's or Dunnett's as needed. A p-value of less than 0.05 indicated statistical significance. Pearson correlation was employed to assess inter-variable relationships. The Shapiro–Wilk test evaluated data normality, and log transformation was applied to non-normal datasets. A 95% confidence interval was used for all statistical assessments [44].

3. RESULTS

3.1. UV–visible spectroscopy

The UV–Vis absorption spectra of the *P. tetrastromatica* extract and the biosynthesized CuO NPs were recorded using a JASCO V-730 UV–Vis spectrophotometer, scanning within a wavelength range of 200–800 nm with 1 nm intervals and a spectral bandwidth of 1.0 nm (Fig. 1). The CuO NPs exhibited a pronounced absorption band at 273 nm, with an absorbance value of 0.547, signifying the presence of surface plasmon resonance (SPR) typical of CuO NPs, confirming their successful synthesis. Conversely, the extract alone did not show any distinct peaks in this region, indicating the transformation of bioactive molecules during nanoparticle formation. A baseline correction was applied during scanning at a rate of 1000 nm/min to improve spectral accuracy. This optical analysis confirms the formation of nanoparticles and distinguishes their optical signature from that of the original biological extract.

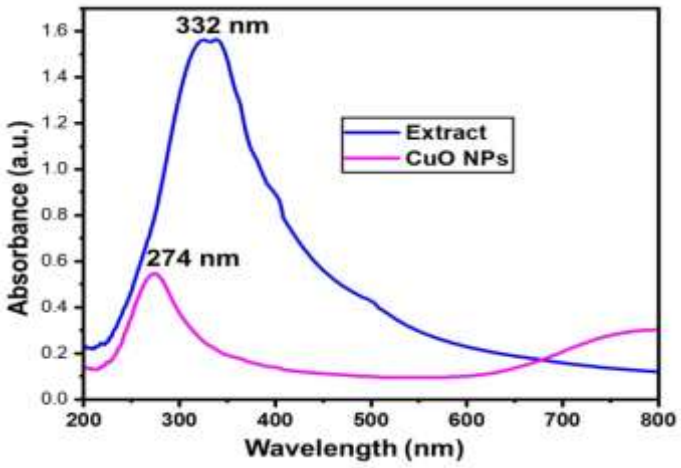

Fig. 1. UV–Visible spectral profiles of algal extract and CuO NPs.

3.2. FTIR spectroscopy analysis

FTIR spectroscopy was conducted using a PerkinElmer Spectrum IR instrument to investigate the molecular structure and bonding of the synthesized materials (Fig. 2). Spectra were recorded between 4000 and 400 cm^{-1}. The CuO NPs displayed prominent peaks at 602.84 cm^{-1} and 433.39 cm^{-1}, which are indicative of Cu–O vibrational modes, validating metal–oxygen bond formation. Additional absorption bands at 3136.73 cm^{-1} (O–H

stretch) and 1654.94 cm^{-1} (C=O stretch) imply residual organic moieties from the algal extract. For the starch/PVA composite nanocomposite, peaks at 3297.44 cm^{-1} (hydroxyl stretching), 1424.21 cm^{-1} (C–H deformation), and 1108.87 cm^{-1} (C–O–C stretching) were observed, corresponding to functional groups from both starch and PVA. Additional signals at 940.79 cm^{-1} and 601.52 cm^{-1} further confirmed the interaction between the polymer and CuO NPs, validating successful nanoparticle loading.

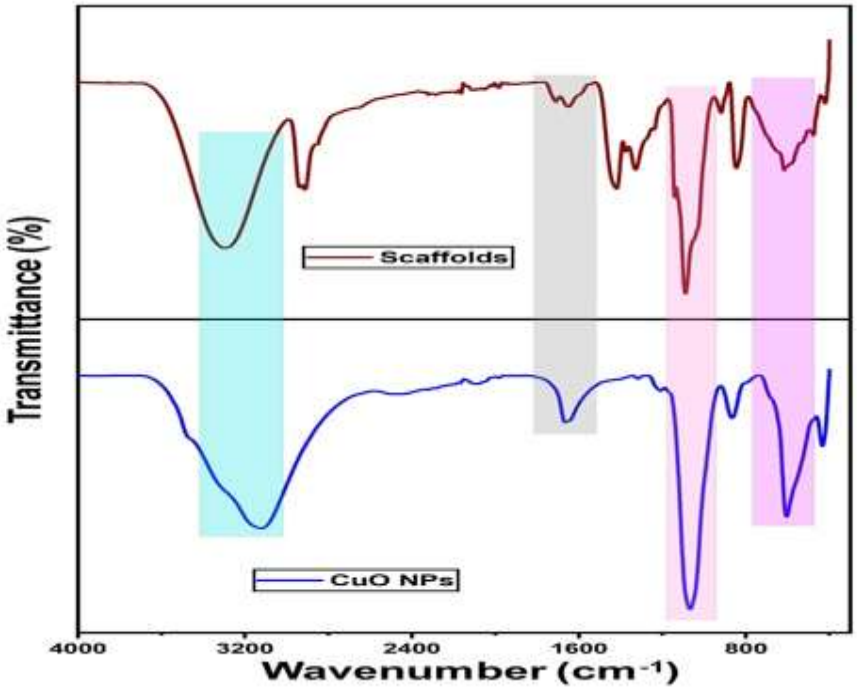

Fig. 2. FTIR spectra of CuO NPs and their incorporation into nanocomposite.

3.3. XRD analysis

The crystallographic properties of the CuO NPs and the electrospun nanocomposite were assessed using a Bruker D8 Advance diffractometer with CuKα radiation (λ = 1.5406 Å) (Fig. 3). The CuO NPs exhibited well-defined peaks between 2θ = 13.310° to 56.302°, corresponding to the monoclinic structure of CuO (tenorite phase) as referenced from JCPDS card no. 05-0661. The most intense reflection appeared at 18.938° with a d-spacing of 4.68228 Å, indicative of high crystallinity. In contrast, the starch/PVA nanocomposite demonstrated a semi-crystalline pattern, with major peaks observed at 21.307° (d = 4.16681 Å) and 29.349° (d = 3.04070 Å), overlaid on broad amorphous humps. Quantitative assessment showed an amorphous content of 82.9% and a crystalline fraction of 17.1%, confirming a composite nature with no extraneous peaks, thereby affirming phase purity.

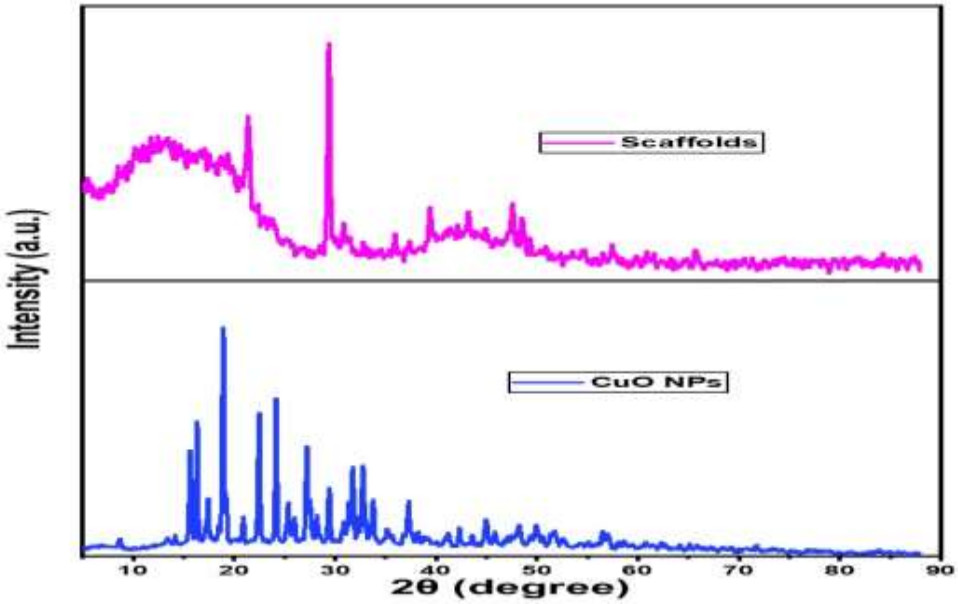

Fig. 3. XRD patterns of synthesized CuO NPs and CuO-loaded scaffolds.

3.4. SEM analysis

SEM imaging was utilized to explore surface topology and nanoparticle dispersion within the nanofibrous matrix (Fig. 4). The CuO NPs appeared as homogeneously scattered particles, ranging from spherical to irregular morphologies. The nanocomposite, fabricated via electrospinning, revealed a porous and interconnected fibrous network structure characterized by smooth, uniform, and bead-free fibers. Embedded CuO NPs were evenly distributed within the polymeric matrix without noticeable agglomeration. The presence of a three-dimensional porous architecture suggests suitability for tissue engineering and wound healing, as it supports gas exchange, nutrient transport, and cellular infiltration—attributes essential for scaffold-based biomedical applications.

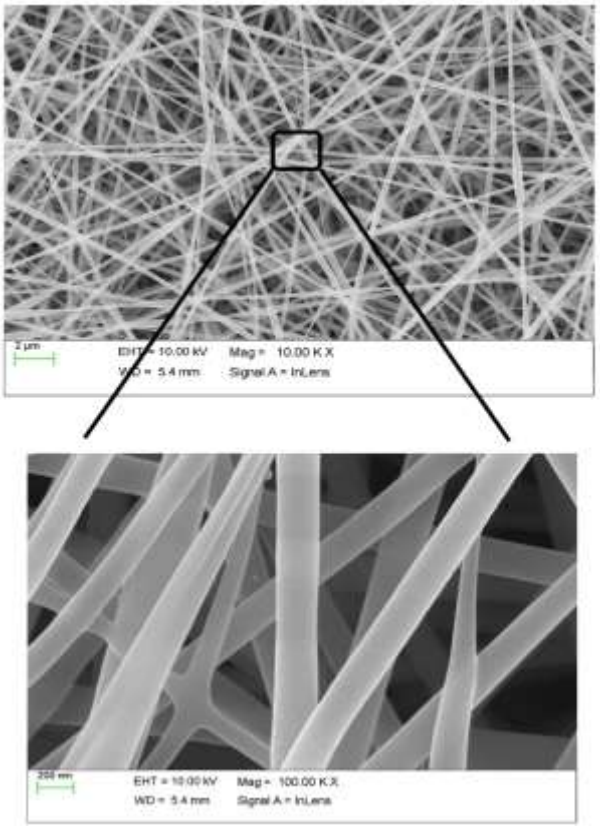

Fig. 4. SEM analysis of synthesized CuO NPs and CuO-loaded scaffolds.

3.5. TGA

The thermal characteristics of the starch/PVA/CuO nanocomposite were studied via TGA using a PerkinElmer analyzer under a nitrogen atmosphere, heating samples from 30°C to 550°C at a constant rate of 15°C/min (Fig. 5). The initial weight loss observed below 150°C is attributed to the evaporation of physically adsorbed water. The major degradation phase began at 298.21°C, peaked at 356.55°C, and ended by 395.85°C, marking the decomposition of organic polymers in the matrix. The total mass loss was recorded at 41.912%, signifying the thermal decomposition of both natural and synthetic polymers. Thermal stability up to approximately 300°C confirms the scaffold's resilience under physiological conditions, aligning with typical thermograms reported for starch and PVA-based nanomaterials.

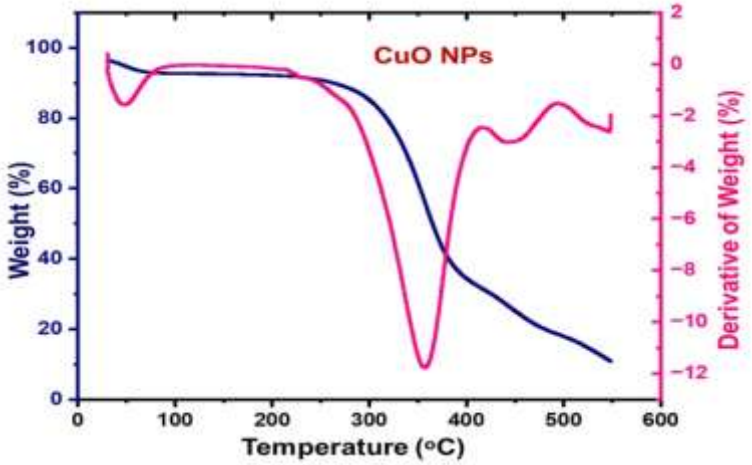

Fig. 5. Thermal degradation behavior of CuO-incorporated nanocomposite.

3.6. Zeta potential and particle size analysis

The colloidal properties of the synthesized CuO NPs were analyzed using DLS and zeta potential measurements via a Malvern Zetasizer Ultra. The DLS analysis indicated that the nanoparticles had a Z-average hydrodynamic diameter of approximately 108 nm (Fig. 6). The surface charge, measured as zeta potential, averaged −22.13 mV, with two notable peaks at −30.51 mV and −16.71 mV (Fig. 7), indicative of a moderately stable colloidal suspension. These negative values suggest the presence of surface-bound functional groups from the algal extract that prevent particle aggregation. The measured conductivity was 0.03211 mS/cm, and the derived count rate was 1570 kcps. Overall, the particle size distribution and zeta potential values support moderate dispersion stability and hint at potential biocompatibility, which are desirable traits for biomedical nanomaterials.

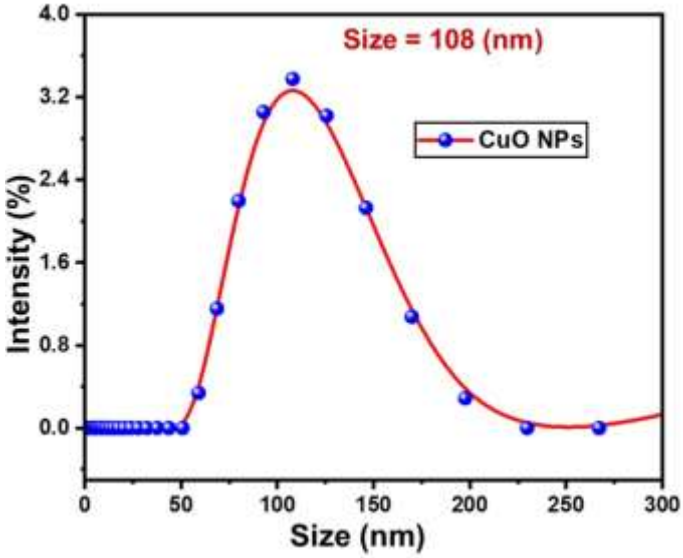

Fig.6. DLS particles size analysis of CuO NPs

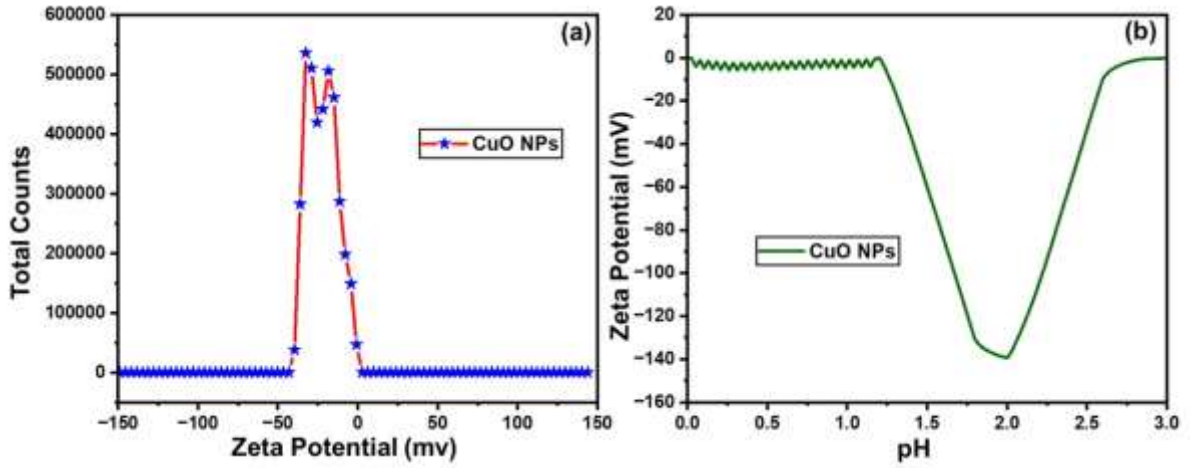

Fig.7. Zeta-potential analysis of CuO NPs

3.7. Wound healing (scratch) assay

The wound healing assay (Fig. 8) demonstrated significant differences in the migratory behavior of HaCaT keratinocyte cells after 48 hours of treatment with algal extract, CuO NPs, and starch/PVA/CuO-NPs nanocomposite. At the lowest concentration (6.25 µg/mL), the algal extract exhibited a wound closure rate of 32.65%, while CuO NPs and nanocomposite showed higher closure rates of 40.65% and 47.65%, respectively. This trend persisted across all concentrations, with the nanocomposite consistently outperforming the other treatments.

At 12.5 µg/mL, the algal extract promoted 39.65% wound closure, whereas CuO NPs and nanocomposite achieved 46.65% and 62.65%, respectively. The superior performance of the nanocomposite became even more pronounced at higher concentrations. At 25 µg/mL, the wound closure rates were 50.65% for the algal extract, 62.65% for CuO NPs, and 73.65% for the nanocomposite.

The highest concentrations (50 and 100 µg/mL) further highlighted the efficacy of the nanocomposite, with closure rates of 79.65% and 95.65%, respectively. In comparison, the algal extract and CuO NPs reached 60.65% and 64.65% at 50 µg/mL, and 69.65% and 83.65% at 100 µg/mL. These results indicate that the starch/PVA/CuO-NPs nanocomposite significantly enhanced keratinocyte migration and wound closure compared to the individual components, suggesting their potential as a promising therapeutic agent for wound healing applications.

The observed differences may be attributed to the synergistic effects of the nanocomposite composite structure, which likely provides a more favorable microenvironment for cell migration and proliferation. In contrast, the algal extract and CuO NPs alone showed moderate efficacy, with CuO NPs performing better than the extract but still lagging behind the nanocomposite. These findings underscore the importance of material composition in designing effective wound healing treatments.

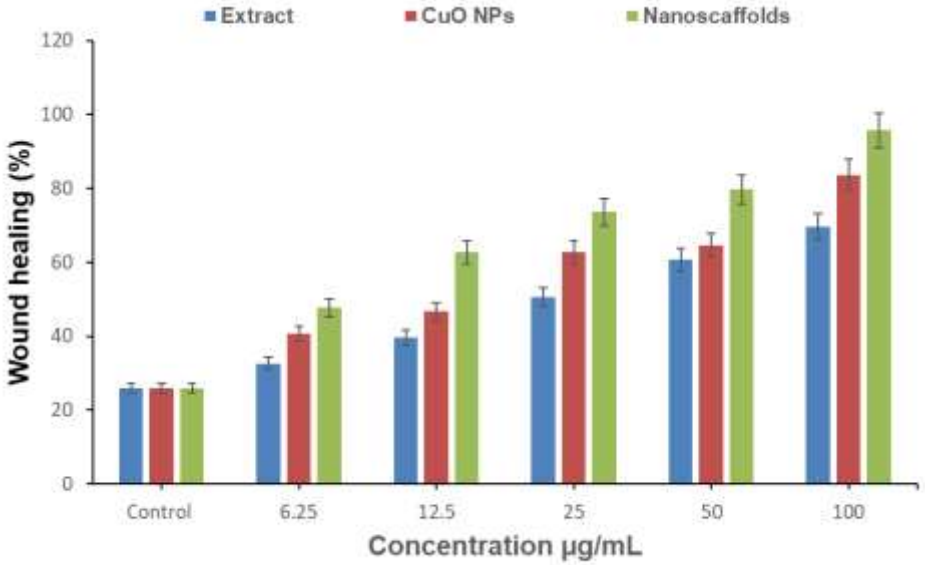

Fig. 8. Wound healing activity analysis of algal extract, CuO-NPs and starch/PVA/CuO-NPs nanocomposite

4. DISCUSSION

The results of this study underscore the successful fabrication, comprehensive physicochemical characterization, and promising wound healing potential of electrospun starch/PVA nanocomposite incorporated with CuO NPs synthesized via ultrasonic-assisted green synthesis using *P. tetrastromatica* extract. Each analytical technique provided insight into the materials' structural, chemical, thermal, and biological performance, establishing their suitability for biomedical applications, particularly in wound care.

The optical properties of the synthesized CuO NPs were evaluated using UV–Visible spectroscopy. A characteristic absorption peak was observed at 273 nm, which is consistent with the surface plasmon resonance (SPR) typically associated with CuO NPs. This confirms the successful reduction of copper ions into stable nanoscale CuO structures, facilitated by phytochemicals in *P. tetrastromatica* extract. Notably, the algal extract alone did not exhibit any sharp peaks, supporting the transformation of its phytoconstituents during nanoparticle formation. The difference in spectral signatures between the extract and the nanoparticles highlights the effectiveness of green synthesis. The baseline correction and consistent scan speed ensured accurate detection, validating the analytical robustness of this approach [45-51].

FTIR analysis revealed key functional groups associated with both the nanoparticles and the nanoscaffold composite. The CuO NPs demonstrated bands characteristic of Cu–O vibrations at around 602 and 433 cm^{-1}, confirming successful metal-oxygen bond formation. Other peaks indicated the retention of organic moieties from the *P. tetrastromatica* extract, which likely played a role in stabilizing the nanoparticles. For the nanocomposite, the spectrum displayed peaks associated with hydroxyl, C–H, and ether linkages, originating from starch and PVA. The presence of additional peaks due to CuO-polymer interactions suggests that the nanoparticles were effectively embedded within the polymer matrix. These findings affirm the composite nature of the nanoscaffold and the compatibility of its constituents [52-59].

XRD patterns provided further confirmation of material composition and crystallinity. The CuO NPs displayed distinct diffraction peaks that matched the monoclinic tenorite phase of CuO, affirming their crystalline structure. The nanocomposite exhibited a combination of sharp and broad peaks, indicating a semi-crystalline structure resulting from the integration of amorphous starch and crystalline PVA components. Quantitatively, the amorphous content was significantly higher (82.9%), which is beneficial for biomedical scaffolds as it often enhances flexibility and biodegradability. Importantly, no extraneous peaks were noted, indicating the high purity of the composite system and the absence of undesirable byproducts [60-64].

SEM images provided crucial insights into the scaffold's surface morphology and nanoparticle distribution. The CuO NPs appeared well-dispersed, ranging from spherical to slightly irregular shapes. Electrospun nanocomposite formed a fibrous mesh with a continuous, bead-free structure and uniform porosity—key attributes for effective wound healing. The uniform integration of CuO NPs within the nanofibers and the absence of aggregation indicate successful fabrication. The observed porous network enhances surface area, promotes oxygen and nutrient

diffusion, and facilitates cellular attachment and migration, making these scaffolds particularly suitable for tissue regeneration [65-71].

The thermal profile of the starch/PVA/CuO nanocomposite demonstrated stability suitable for biomedical use. The initial mass loss below 150°C was due to moisture evaporation, while the main degradation phase occurred between approximately 298°C and 396°C. This major mass loss corresponds to the breakdown of the organic polymeric matrix. A total weight loss of 41.912% was recorded, which is within the expected range for natural-synthetic polymer composites. The data affirm that the scaffolds can maintain their structural integrity under physiological and mild thermal stress, which is essential for safe *in vivo* applications [72-75].

Colloidal stability and particle size distribution were evaluated using DLS and zeta potential measurements. The average hydrodynamic diameter of CuO NPs was 108 nm, falling within the optimal nanoscale range for biomedical delivery and tissue interaction. The zeta potential value of −22.13 mV, with subpopulations at −30.51 mV and −16.71 mV, suggests moderate stability of the nanoparticle suspension. While values beyond ±30 mV typically indicate strong electrostatic repulsion, the observed negative charge still points to surface functionalization that prevents excessive aggregation. These findings suggest that the nanoparticles are stable enough for biomedical applications and may exhibit favorable bioavailability and reduced toxicity [76-78].

The wound healing assay results demonstrated the superior efficacy of starch/PVA/CuO-NPs nanocomposite in promoting keratinocyte migration compared to both the *P. tetrastromatica* extract and CuO NPs alone. Across all tested concentrations (6.25 to 100 µg/mL), the nanoscaffold-treated groups consistently exhibited higher wound closure percentages. At the highest concentration, the nanocomposite achieved an impressive 95.65% wound closure, compared to 83.65% for CuO NPs and 69.65% for the extract. This enhanced performance can be attributed to the synergistic effects of the composite structure, where the scaffold provides a biocompatible and supportive matrix while the CuO NPs deliver localized antimicrobial and regenerative stimuli. The porous architecture likely plays a pivotal role in facilitating cellular infiltration and nutrient exchange, crucial for efficient wound repair [79].

Collectively, the integration of biosynthesized CuO NPs into starch/PVA electrospun nanocomposite produced a multifunctional biomaterial with excellent physicochemical properties and notable wound healing capabilities. The findings affirm the potential of these green-fabricated nanocomposite in advanced biomedical applications, particularly as effective wound dressings that can enhance tissue regeneration while maintaining biocompatibility and thermal stability.

5. CONCLUSION

This study successfully demonstrated the green synthesis of CuO NPs using *P. tetrastromatica* extract and their incorporation into starch/PVA nanocomposite for enhanced wound healing applications. Spectroscopic and microscopic analyses confirmed the formation of crystalline, stable CuO NPs with uniform dispersion within the nanofibrous scaffold matrix. The nanocomposite exhibited favorable physicochemical properties, including thermal stability, porous architecture, and colloidal integrity, making them suitable for biomedical applications. The wound healing assay revealed that the starch/PVA/CuO-NP nanocomposite significantly outperformed both the algal extract and CuO NPs alone, achieving up to 95.65% wound closure at 100 µg/mL. This enhanced efficacy can be attributed to the synergistic effects of the composite structure, which promotes cell adhesion, migration, and proliferation. The nanocomposite' three-dimensional fibrous network likely mimics the extracellular matrix, facilitating tissue regeneration. These findings highlight the potential of *P. tetrastromatica*-mediated CuO NPs embedded in starch/PVA nanocomposite as an advanced, biocompatible wound dressing material. Future studies should explore *in vivo* performance and long-term biocompatibility to further validate their clinical applicability in regenerative medicine.

Ethical Declaration: Not Applicable

Data Availability Statement: The full dataset of physiochemical characterization associated with this work is published in Mendeley Data [Dataset] Padina tetrastromatica-driven synthesis meets biopolymers: comprehensive profiling of starch nanoscaffolds infused with eco-friendly copper oxide nanoparticles (DOI: 10.17632/ddbgcpm32x.1). Disclosure: The material characterization data and figures (e.g., UV, SEM, FTIR, XRD, TGA, Zeta Potential and particle sizer) presented here were generated from a common dataset and are being reused across multiple related studies on nanomaterials. All biological analyses and conclusions are original to each manuscript.

Conflicts of Interest: The authors declare no conflicts of interest.

REFERENCES

[1] Sakthiraj A, Sivaramakrishnan R, Subramaniyam S, Kanniappan GV, Pandurangan V, Jayaraman S, Dhayalan VK, Mironescu M, Mironescu ID, Palanisamy CP. Starch/PVA electrospun nanoscaffolds loaded with ultrasonic-assisted green-synthesis of CuO nanoparticles from marine macroalgae (Gracilaria corticata) extract: Cytotoxicity and antioxidant analysis. Chemical Physics Impact. 2026; 12: 101018.

[2] Raju M, Chandrasekaran MK, Loganathan L, Ahalliya RM, Mironescu M, Mironescu ID, Palanisamy CP, Kanniappan GV. Lipid remodeling and ferroptosis in phosphatidylcholine-mediated tumor–stroma crosstalk. Frontiers in Molecular Biosciences. 2026; 13: 1742305.
[3] Kunamalla R, Panagal M, Palanisamy CP. Biogenic synthesis and fabrication of starch/PVA/CuO electrospun nanoscaffolds from Sargassum ilicifolium (brown marine macroalgae) extract for anticancer activity on HT-29 and MCF-7 cancer cells. Biocatalysis and Agricultural Biotechnology. 2026; 72: 103923.
[4] Pei J, Govindaraj H, Sivaramakrishnan R, Kanniappan GV, Pandurangan V, Dhayalan VK, Mironescu M, Mironescu ID, Jayaraman S, Palanisamy PC. Sustainable fabrication of biopolymer-based (starch/PVA) nanoscaffolds loaded with green-synthesized CuO nanoparticles from Sargassum wightii (marine macroalgae): Cytocompatibility and antioxidant activity. Biomaterials Advances. 2026; 182: 214660.
[5] Pei J, Perumal NC, Meng P, Long Q, Palanisamy CP. Extracellular vesicle-based biosensors for Alzheimer's disease: A new frontier in precision diagnostics. Ageing Research Reviews. 2026; 113: 102904.
[6] Shree P, Sivaramakrishnan R, Kanniappan GV, Pandurangan V, Jayaraman S, Dhayalan VK, Mironescu M, Mironescu ID, Palanisamy CP. Antioxidant and biocompatible CuO-starch/PVA nanoscaffolds via ultrasonic green synthesis using Turbinaria conoides (brown marine macroalgae). Medicine in Drug Discovery. 2025; 28: 100238.
[7] Gong J, Lin J, Guan T, Pei J, Palanisamy CP, El-AtyFrom AMA. selenium tolerance to nanoplastic antagonism: Comprehensive characterization of L. casei SNUT1 and its extracellular vesicle–nanoselenium complex. Food Bioscience. 2025; 74: 107749.
[8] Poochi SP, Sundarraj R, Raju MV, Chandrasekaran MK, Ahalliya RM, Palanisamy CP, Kanniappan GV, Kondapavuluri BK, Thiruvengadam M. Harnessing Nature: Computational and Experimental Insights Into *Ipomoea obscura* Metabolites for Bladder Cancer Therapy. Chemistry and Biodiversity. 2025; 0: e00909.
[9] Dugganaboyana GK, Kannankumar MKG, Shivaramakrishna S, Raju MV, Chandrasekaran MK, Ahalliya RM, Panneerselvam N, Palanisamy CP, Kanniappan GV. Phytochemical insights, antioxidant activity and therapeutic potential of Cassia senna against prostate cancer in Wistar albino rats. Discover Applied Sciences. 2025; 7:1206.
[10] Natarajan SR, Krishnamoorthy R, Alshuniaber MA, Gatasheh MK, Rajagopal P, Veeraraghavan VP, Palanisamy CP, Jayaraman S. KDM1A Facilitates Oncogenic Potential in Colorectal Cancer Progression Through the Activation of AXIN/GSK3β/β-Catenin Signaling Pathways: Evidence From Integrated Transcriptomics and In Vitro Studies. The Journal of Gene Medicine. 2025; 27(11): e70053.
[11] Guan T, Gong J, Lin J, Palanisamy CP, Jinjin Pei J, El-Aty AMA. Machine learning-driven multimodal optimization of selenium biotransformation and flavor profiling in fermented apple–Yacon functional beverages. Innovative Food Science & Emerging Technologies. 2025; 105: 104198.
[12] Natarajan SR, Krishnamoorthy R, Alshuniaber MA, Alsulami TS, Gatasheh MK, Rajagopal P, Palanisamy CP, Govindan R, Veeraraghavan VP, Jayaraman S. ABCE1 facilitates tumour progression via aerobic glycolysis and inhibits cell death in human colorectal cancer cells through the p53 signalling pathway. Scientific Reports. 2025; 15: 24674.
[13] Huang Y, Guo H, Liu Y, Jin W, Palanisamy CP, Pei J, Oz F, El-Aty AMA. Effects of Natural Polysaccharides on the Gut Microbiota Related to Human Metabolic Health. Molecular Nutrition & Food Research. 2025; 69:e202400792.
[14] Poornima K, Meenakshi K.C, Manikandan V.R, Shankari G, Prabhu D, Rathi M.A, Palanisamy CP, Balaji R, Gopalakrishnan V.K. Exploring the anticancer potential of Jerantinine A from *Tabernaemontana coronaria* against prostate, breast, and ovarian cancers: A computational approach. *Journal of Complementary and Integrative Medicine*, 2025 22(2): 363–372.
[15] Palanisamy CP, Poompradub S, Sansanaphongpricha K, Jayaraman S, Subramani K. Faridah Sonsudin gGreen synthesis of Nigella sativa-mediated silver nanoparticles for enhanced antibacterial activity and wound healing: Mechanistic insights and biomedical applications. Environmental Nanotechnology, Monitoring & Management. 2025; 24: 101085.
[16] Surendran N, Raju MV, Chandrasekaran MK, Ahalliya RM, Palanisamy CP, Chandrasekaran G, Kanniappan GV. Physicochemical characterization of starch from Maranta arundinacea L.(arrowroot) rhizomes and its inhibition of COX-2: In vivo validation. Bioactive Carbohydrates and Dietary Fibre. 2025; 33: 100465.
[17] Natarajan PM, Swamikannu B, Sivaraman NM, Stylin AGSQ. Prevention of Oral Cancer: A Comprehensive Guide. Journal of Pharmacy and Bioallied Sciences. 2024; 16(5): S4239-S4241.
[18] Umapathy V, Dhanavel A, Kesavan R, Natarajan PM, Bhuminathan S, Vijayalakshmi P. Anticancer Potential of the Principal Constituent of Piper nigrum, Piperine: A Comprehensive Review. Cureus. 2024; 16(2): e54425.
[19] Umapathy VR, Swamikannu B, Natarajan PM, Devi R, Nandini MS, Vimalarani, Vijayalakshmi P. In Silico Molecular Docking of Ocimum sanctum Phytochemicals: Targeting Key Biomarkers in Oral Cancer. Journal of Pharmacy and Bioallied Sciences. 2024; 16(5): S4792-S4799.
[20] Natarajan PM, Bhuminathan S, Rajan R, Bindu K, Loganathan K, Veerakumar R. The Crucial Role of Smoking Cessation in Preventing Oral Cancer. Journal of Pharmacy and Bioallied Sciences. 2024; 16(5): S4245-S4247.

[21] Swamikannu B, Umapathy VR, Natarajan PM, Nandini MS, Stylin AGSQ, Vimalarani V, Rajinikanth S. Unlocking the Therapeutic Benefits of Artemisia Annua: A Comprehensive Overview of its Medicinal Properties. Journal of Pharmacy and Bioallied Sciences. 2024; 16(5): S4248-S4253.
[22] Natarajan PM. Computational Studies on Recent Congeners of Fluoroquinolones and Nitroimidazoles for Their Use in Periodontal Therapy. Journal of Pharmacy and Bioallied Sciences. 2024; 16(5): S4731-S4740.
[23] Yadalam PK, Arumuganainar D, Natarajan PM, Ardila CM. Artificial intelligence-powered prediction of AIM-2 inflammasome sequences using transformers and graph attention networks in periodontal inflammation. Scientific Reports. 2025; 15: 8733.
[24] Yadalam PK, Chatterjee S, Natarajan PM, Ardila CM. Comparison of light gradient boosting and logistic r egression for interactomic hub genes in Porphyromonas gingivalis and Fusobacterium nucleatum-induced perio dontitis with Alzheimer's disease. Frontiers in Oral Health. 2025; 6:1463458.
[25] Natarajan PM, Bhuminathan S, Leela B, Bindu K, Loganathan K, Ramachandran V. Smoking and its Role in Oral Cancer. Journal of Pharmacy and Bioallied Sciences 16(5): S4242-S4244.
[26] Yadalam PK, Natarajan PM, Ardila CM. Variational graph autoencoder for reconstructed transcriptomic data associated with NLRP3 mediated pyroptosis in periodontitis. Scientific Reports. 2025; 15: 1962.
[27] Pei JJ, Perumal NC, Meng P, Long Q, Palanisamy CP. AI-assisted FTIR spectroscopic profiling of exosomes: Emerging frontiers in early detection of Alzheimer's disease. Ageing Research Reviews. 2026; 103311.
[28] Raja FSD, Abraham L, Rangasamy K, Saikia K, Rathankumar AK, Mironescu M, Mironescu I, Palanisamy CP, Kanniappan GV. Next-Generation Microbiome Therapeutics: Psychobiotics and Fecal Microbiota Transplants (FMT) for Mental Health Treatment. Frontiers in Cellular and Infection Microbiology. 2026; 16: 1719357.
[29] Subramani K, Srinivasan S, Shanmugam P, Palanisamy CP, Sonsudin F, Poompradub S. Sustainable phytochemical mediated-ZnO nanoparticles derived from Crescentia cujete for toxicological evaluation and multifunctional environmental applications. Environmental Nanotechnology, Monitoring & Management. 2026; 26: 101180.
[30] Kunamalla RP, Panagal M, Palanisamy CP. Green-engineered multiscale starch/PVA nanofibrous scaffolds embedded with CuO nanoparticles from Sargassum ilicifolium for potent antimicrobial performance. Genetics and Molecular Research. 2026; 25(13s): 1-9.
[31] Dharmaprakash S, Gunasekaran VP, Sivaramakrishnan R, Kanniappan GV, Jayaraman S, Mironescu M, Rajabathar JR, Mironescu ID, Palanisamy CP. Marine macroalgae-mediated ultrasonic-assisted green synthesis of CuO nanoparticles embedded in starch/PVA electrospun nanoscaffolds for in vitro α-amylase and α-glucosidase inhibitory activity. Scientific Reports. 2026; 16: 26243.
[32] Surendran N, Chandrasekaran G, Raju MV, Chandrasekaran MK, Ahalliya RM, Palanisamy CP, Kanniappan GV, Arcot R, Alharbi NS, Thiruvengadam M. Anti-inflammatory potential of ethanolic extract of Maranta arundinacea L.: Insights from COX-2 modulation and oxidative stress analysis. South African Journal of Botany. 2026; 195: 142-151.
[33] Pei J, Senthilkumar MV, Hessini K, Subramaniyam S, Sivaramakrishnan R, Kanniappan GV, Jayaraman S, Palanisamy CP. Green fabrication of starch/PVA/CuO nanoscaffolds using marine macroalgae extract for enhanced anti-inflammatory activity. Sustainable Chemistry and Pharmacy. 2026; 51: 102397.
[34] Balasubramanian V, Loganathan L, Muthuswamy K, Viswanathan TM, Raju MV, Chandrasekaran MK, Ahalliya RM, Poorasamy J, Palanisamy CP, Dominic S, Kanniappan GV. Anticancer therapeutic efficacy of PEGylated β-galactosidase from Aspergillus terreus in DMBA-induced breast cancer: Toxicological, molecular and histopathological evaluation in Wistar rats. International Journal of Biological Macromolecules. 2026; 360: 151856.
[35] Jayaraman S, Eswaran A, Rajagopal P, Palanisamy CP, Veerakumar P, Veeraraghavan VP, Sirasanagandla SR. Neuroendocrine-associated epigenetic factors in cellular senescence: mechanisms and therapeutic implications. Biogerontology. 2026; 27(2): 64.
[36] Ponnusamy B, Rajagopal P, Palanisamy CP, Veeraraghavan VP, Jayaraman S. Mechanistic Exploration of the anticancer activity of Justicia adhatoda Plant Leaf Ethanolic Extract against Colon Cancer Cells: An in silico and in vitro Approach. Asian Pacific Journal of Cancer Prevention. 2026; 27(3): 1069-1080.
[37] Pei J, Saran VS, Sivaramakrishnan R, Kanniappan GV, Pandurangan V, Jayaraman S, Dhayalan VK, Mironescu M, Mironescu ID, Palanisamy CP. Ultrasonic-assisted, Sargassum ilicifolium (brown marine macroalgae)-mediated biogenic synthesis of CuO nanoparticles incorporated in starch/PVA electrospun nanoscaffolds: In vitro safety and antioxidant efficacy assessment. Bioorganic Chemistry. 2026; 173: 109679.
[38] Raj MAPA, Subramaniyam S, Kanniappan GV, Jayaraman S, Palanisamy CP. Sustainable fabrication of starch/PVA/CuO electrospun nanoscaffolds from Turbinaria ornata (marine macroalgae) extract: Physicochemical characterization and antidiabetic evaluation. Kuwait Journal of Science. 2026; 53(2): 100545.
[39] Pei J, Ganesh NS, Subramaniyam S, Sivaramakrishnan R, Kanniappan GV, Jayaraman S, Palanisamy CP. Sustainable fabrication of starch/PVA/CuO electrospun nanoscaffolds from Padina tetrastromatica (Brown macroalgae) extract: Physicochemical characterization and antidiabetic assessment. Sustainable Chemistry One World. 2026; 9: 100195.

[40] Natarajan PM, Umapathy VR, Murali A, Swamikannu B. (2022). Computational Simulations of Identified marine-derived Natural Bioactive Compounds As Potential Inhibitors of Oral Cancer. Future Science OA. 2022; 8(3).
[41] Natarajan PM, Umapathy VR. Role of transcriptomics in the study of oral cancer. Frontiers in Oral Health. 2025; 6:1524364.
[42] Vidhyarekha U, Natarajan PM, Bhuminathan S, Sabarinathan J, Suba R, Vijayalakshmi P. Role of artificial intelligence in Oral Cancer. Advances in Public Health. 2024. 2024: 3664408.
[43] Ganesan A, Kumar NG, Natarajan PM, Gauthaman J. Automated classification of elongated styloid processes using deep learning models-an artificial intelligence diagnostics. Frontiers in Oral Health. 2025; 5: 1424840.
[44] Umapathy VR, Natarajan PM, Swamikannu B. Regenerative Strategies in Dentistry: Harnessing Stem Cells, Biomaterials and Bioactive Materials for Tissue Repair. Biomolecules. 2025; 15: 546.
[45] Natarajan PM. Dental Bioinformnatics-Current Scope and Future perspectives. Research Journal of Pharmacy and Technology. 2022;15(5):2351-6.
[46] Ganesan A, Kumar NG, Natarajan PM. Solanum trilobatum leaf extract-derived silver nanoparticles downregulate the PI3K/AKT/mTOR signaling pathway and attenuate oral squamous cell carcinoma cell proliferation. Journal of Herbmed Pharmacology. 2024; 13(2): 300-307.
[47] Perumal MKK, Renuka RR, Subbiah SK, Natarajan PM. Artificial intelligence-driven clinical decision support systems for early detection and precision therapy in oral cancer: a mini review. Frontiers in Oral Health. 2025; 6: 1592428.
[48] Ramesh E, Ganesan A, Lakshmi KC, Natarajan PM. Artificial intelligence-based diagnosis of oral leukoplakia using deep convolutional neural networks Xception and MobileNet-v2. Frontiers in Oral Health. 2025; 6: 1414524.
[49] Ganesan A, Kumar NG, Natarajan PM. Anticancer activity of silver nanoparticles synthesized from aqueous leaf extract of Solanum trilobatum (Purple fruit pea eggplant) on human oral cancer cells. Journal of Herbmed Pharmacololgy. 2024; 13(2): 260-268.
[50] Kannappan P, Chandrasekaran MK, Raju MV, Gopalakrishnan S, Dhamodharan P, Ahalliya RM, Palanisamy CP, Raju B, Kanniappan GV. Exploring the anticancer potential of Jerantinine A from Tabernaemontana coronaria against prostate, breast, and ovarian cancers: a computational approach. Journal of Complementary and Integrative Medicine. 2025; 22(02): 363-372.
[51] Pei J, Kumarasamy RV, Jayaraman S, Kanniappan GV, Long Q, Palanisamy CP. Quercetin-functionalized nanomaterials: Innovative therapeutic avenues for Alzheimer's disease management. Ageing Research Reviews. 2025; 104: 102665.
[52] Jayaraman S, Prasad M, Natarajan SR, Krishnamoorthy R, Alshuniaber MA, Gatasheh MK, Veeraraghavan VP, Rajagopal P, Palanisamy CP. Molecular mechanisms underlying the effects of beta-sitosterol on TGF-β1/Nrf2/SIRT1/p53-mediated signaling in the kidney of a high-fat diet and sucrose-induced type-2 diabetic rat. Chemico-Biological Interactions. 2025; 411: 111443.
[53] Huang Y, Guo H, Liu Y, Jin W, Palanisamy CP, Pei J, Oz F, El-Aty AMA. Effects of Natural Polysaccharides on the Gut Microbiota Related to Human Metabolic Health. Molecular Nutrition & Food Research. 2025; e202400792.
[54] Prabhakaran P, Palanisamy CP, Shanmugam A, Damodharan P, Swaminathan H, Devaraj D, Ahalliya RM, Kanniappan GV. Isolation, structural characterization, and molecular docking studies on the bioactive compound from n-Hexane extract of Emilia sonchifolia (L.) DC against the pancreatic cancer target Aurora 2 Kinase. Journal of Complementary and Integrative Medicine. 2024; 22(1): 0290.
[55] Jiang H, Kumarasamy RV, Pei J, Raju K, Kanniappan GV, Palanisamy CP. Integrating engineered nanomaterials with extracellular vesicles: Advancing targeted drug delivery and biomedical applications. Frontiers in Nanotechnology. 2024; 6: 1513683.
[56] Guo H, Liu Y, Wan T, Song D, Palanisamy CP, Geng J, Pei J, Özmen S, El-Aty AMA. Toward personalized cancer management: Role of precision nutrition–diet interventions. Journal of Functional Foods. 2024; 123: 106584.
[57] Natarajan SR, Krishnamoorthy R, Alshuniaber MA, Al-Anazi KM, Farah MA, Rajagopal P, Palanisamy CP, Veeraraghavan VP, Jayaraman S. Identification of FOXM1 as a novel protein biomarker and therapeutic target for colorectal cancer progression: Evidence from immune infiltration and bioinformatic analyses. International Journal of Biological Macromolecules. 282 (Part 4): 137201.
[58] Rajendran MS, Jayaraman S, Khan JM, Jasmine S, Prabhakaran RK, Raju MV, Chandrasekaran MK, Ahalliya RM, Kannappan P, Palanisamy CP, Kanniappan GV. Investigating the colon toxicity and carcinogenic role of monosodium glutamate compared with Dimethylhydrazine in male Wistar rats: Exploring the link to childhood colon cancer risk. Journal of King Saud University - Science. 2024; 36(11): 103507.
[59] Kumarasamy RV, Natarajan P, Umapathy VR, Roy JR, Rab SO, Saeed M, Panagal M, Mironescu M, Srinivasan GP, Palanisamy CP. Clinical Applications and Therapeutic Potentials of Advanced Nanoparticles: A Comprehensive Review on Completed Human Clinical Trials. Frontiers in Nanotechnology. 2024; 6:1479993.

[60] Jin W, Pei JJ, Roy JR, Jayaraman S, Ahalliya RM, Kanniappan GV, Mironescu M, Palanisamy CP. Comprehensive review on single-cell RNA sequencing: A new frontier in Alzheimer's disease research. Ageing Research Reviews. 2024; 274: 102454.
[61] Pei J, Palanisamy CP, Jayaraman S, Natarajan PM, Umapathy VR, Roy JR, Panagal M, Jayaraman S. Curcumin-loaded polymeric nanomaterials as a novel therapeutic strategy for Alzheimer's disease: A comprehensive review. Ageing Research Reviews. 2024; 99: 102393.
[62] Pei J, Palanisamy CP, Jayaraman S, Natarajan PM, Umapathy VR, Roy JR, Thalamati D, Ahalliya RM, Kanniappan GV, Mironescu M. A comprehensive review on starch-based Sustainable Edible Films Loaded with Bioactive Components for Food Packaging. International Journal of Biological macromolecules. 2024; 274 (Part-1): 133332.
[63] Palanisamy CP, poompradub S, Sansanaphongpricha K, Subramani K, Sonsudin F. Increased expression levels of PDGF and VEGF magnify the wound healing potential facilitated by biogenic synthesis of silver nanoparticles. Nano-Structures & Nano-Objects. 2024; 39: 101236.
[64] Pei J, Palanisamy CP, Jayaraman S, Natarajan PM, Umapathy VR, Roy JR, Thalamati D, Ahalliya RM, Kanniappan GV, Mironescu M. Proteomics Profiling of Extracellular Vesicle for Identification of Potential Biomarkers in Alzheimer's Disease: A Comprehensive Review. Ageing Research Reviews. 2024; 99: 102359.
[65] Xi J, Wang T, Xian P, Liu X, Du M, Yang H, Palanisamy CP, Lin W, Long Q. Proteomic insights uncover enhanced neurotherapeutic potential in conditioned mesenchymal stem cell-derived extracellular vesicles. Extracellular Vesicle. 2024; 3: 100037.
[66] Pei J, Natarajan PM, Umapathy VR, Swamikannu B, Sivaraman NM, Krishnasamy L, Palanisamy CP. Advancements in the synthesis and functionalization of zinc oxide-based nanomaterials for enhanced oral cancer therapy. Molecules. 2024; 29(11): 2706.
[67] Gatasheh MK, Natarajan SR, Krishnamoorthy R, Alsulami TS, Rajagopal P, Palanisamy CP, Veeraraghavan VP, Jayaraman S. Molecular analysis to identify novel potential biomarkers as drug targets in colorectal cancer therapy: an integrated bioinformatics analysis. Molecular and Cellular Oncology. 2024; 11(1): 2326699.
[68] Pei J, Yan Y, Jayaraman S, Rajagopal P, Natarajan PM, Umapathy VR, Gopathy S, Roy JR, Sadagopan CS, Thalamati D, Palanisamy CP, Mironescu M. A review on advancements in the application of starch-based nanomaterials in biomedicine: Precision drug delivery and cancer therapy. International Journal of Biological Macromolecules. 2024; 130746.
[69] Pei JJ, Yan Y, Palanisamy CP, Jayaraman S, Natarajan PM, Umapathy VR, Gopathy S, Roy JR, Sadagopan JC, Thalamati D, Mironescu M. Materials-based drug delivery approaches: Recent advances and future perspectives. Green Processing and Synthesis. 2024; 13: 20230094.
[70] Pei JJ, Deng W, Liu Y, Guo Y, Chen J, Abdu H, Khan MR, Palanisamy CP, El-Aty AM. A Comprehensive Review of Cornus officinalis: Health Benefits, Phytochemistry, and Pharmacological Effects for Functional Drug and Food Development. Frontiers in Nutrition. 2023; 10: 1309963.
[71] Alugoju P, Palanisamy CP, Anthikapalli NVA, Jayaraman S, Prasanskulab A, Chuchawankul S, Dyavaiah M, Tencomnao T. Exploring the anti-aging potential of natural products and plant extracts in budding yeast Saccharomyces cerevisiae: A review. F1000Research. 2023; 12: 1265.
[72] Lavanya M, Krishnamoorthy R, Alshuniaber MA, Manoharadas S, Palanisamy CP, Veeraraghavan VP, Jayaraman S, Rajagopal P, Padmini R. Formulation, characterization and evaluation of gelatin-syringic acid/zinc oxide nanocomposite for its effective anticancer, antioxidant and anti-inflammatory activities. Journal of King Saud University-Science. 2023; 35: 102909.
[73] Palanisamy CP, Poompradub S, Sansanaphongpricha K, Jayaraman S, Subramani K, Sonsudin F. Biosynthesis of silver nanoparticles (AgNPs) using ethanolic extract of Nigella sativa (L.) seeds promotes wound healing via PDGF and VEGF signalling pathways activation. Biocatalysis and Agricultural Biotechnology. 2023; 54: 102970.
[74] Prasad M, Jayaraman S, Natarajan SR, Veeraraghavan VP, Krishnamoorthy R, Gatasheh MK, Palanisamy CP, Elrobh M. Piperine modulates IR/Akt/GLUT4 pathways to mitigate insulin resistance: Evidence from animal and computational studies. International Journal of Biological Macromolecules. 2023; 253: 127242.
[75] Palanisamy CP, Pei JJ, Phaniendra A, Venkata AAN, Jayaraman S, Veeraragahavan VP, Sridevi G, Roy JR, Janaki CS, Thalamati D, Mironescu M, Luo Q, Chai Y, Long Q. New Strategy of Neurodegenerative Disease Treatment with Extracellular Vesicles (EVs) Derived from Mesenchymal Stem Cells (MSCs). *Theranostics*. 2023; 13(12):4138-4165. doi:10.7150/thno.83066.
[76] Palanisamy CP, Phaniendra A, Jayaraman S, Poompradub S. *Nigella sativa* L. seed extracts promotes wound healing progress by activating VEGF and PDGF signalling pathways: *An in vitro* and *in silico* study. *F1000 Research*. 2023; 12: 436.
[77] Pei JJ, Palanisamy CP, Phaniendra A, Venkata AAN, Natarajan PM, Umapathy VR, Swamikannu B, Jayaraman S, Rajagopal P, Poompradub S. A comprehensive review on bio-based materials for chronic diabetic wounds. *Molecules*. 2022; 28(2), 604.
[78] Palanisamy CP, Cui B, Zhang H, Gunasekaran VP, Ariyo A, Jayaraman S, Veeraraghavan V, Rajagopal P. A critical review on starch-based electrospun nanofibrous scaffolds for wound healing application. International Journal of Biological Macromolecules. 2022; 222 (Part: B): 1852-1860.